Available online at www.sciencedirect.com
ScienceDirect
Bioorganic & Medicinal Chemistry Letters 18 (2008) 3359–3363
Bioorganic & Medicinal Chemistry Letters

Synthesis and structure based optimization of novel Akt inhibitors

Blaise Lippa,* Gonghua Pan, Matthew Corbett, Chao Li, Goss S. Kauffman, Jayvardhan Pandit, Shaughnessy Robinson, Liuqing Wei, Ekaterina Kozina, Eric S. Marr, Gary Borzillo, Elisabeth Knauth, Elsa G. Barbacci-Tobin, Patrick Vincent, Merin Troutman, Deborah Baker, Francis Rajamohan, Shefali Kakar, Tracey Clark and Joel Morris*

Pfizer, Inc., PGRD Groton, 558 Eastern Point Road, Groton, CT 06340, USA

Received 6 March 2008; revised 8 April 2008; accepted 10 April 2008
Available online 15 April 2008

Abstract—Based on a high throughput screening hit, pyrrolopyrimidine inhibitors of the Akt kinase are explored. X-ray co-crystal structures of two lead series results in the understanding of key binding interactions, the design of new lead series, and enhanced potency. The syntheses of these series and their biological activities are described. Spiroindoline **13j** is found to have an Akt1 kinase IC_{50} of 2.4 ± 0.6 nM, Akt cell potency of 50 ± 19 nM, and provides 68% inhibition of tumor growth in a mouse xenograft model (50 mg/kg, qd, po).

The serine/threonine kinase Akt (PKB) is a key signaling component in the IGF-1R/PI3K/PTEN cell survival pathway.[1–4] It was initially identified as a fusion protein in an oncogenic retrovirus (AKR mouse Thymoma), and was subsequently shown to have oncogenic potential in cell transformation assays. Three Akt genes exist in humans: AKT1, AKT2, and AKT3.

Multiple observations point to Akt as an important cancer drug discovery target,[5] including: (i) the tumor suppressor PTEN, a negative regulator of Akt kinase activity, is mutated or deleted at high frequency in solid human cancers and several cancer susceptibility syndromes[6]; (ii) Akt is activated via growth factor receptors and/or ligands that are up-regulated in a wide variety of solid human tumors, and (iii) AKT gene amplification has been reported in several cancer lines.[7,8]

Based on the strong rationale for inhibiting Akt as a therapy for cancer, there have been multiple efforts to discover small molecule antagonists.[9,10] These have included both allosteric inhibitors,[11,12] and inhibitors designed to bind in the enzyme active site in competition with ATP.[13–19]

At Pfizer, a high throughput screen revealed that pyrrolopyrimidine **1** was a 290 nM inhibitor of Akt1 in an in vitro kinase assay (Fig. 1).[20] To further explore the SAR of this lead, multiple analogs were synthesized (Scheme 1). Condensation of 4-hydrazinoquinazolines (**2**) with orthoformates followed by ring opening with aqueous KOH provided anilinotriazole **3**.[21] The aniline was then added to a chloropyrrolopyrimidine (**4**)[22] in 1,2-dichloroethane resulting in the completed analogs (**5**).

The resulting compounds were assayed for the inhibition of Akt1 (Table 1).[20] Methyl substitution of the pyrrole

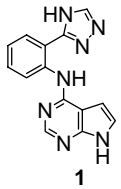

1

Akt1 kinase IC_{50} = 210 +/- 66 nM

Figure 1. Structure and Akt1 kinase potency of high throughput screen hit.

Keywords: Akt; Pyrrolopyrimidine; Spiroindoline; Imidazopiperidine.
* Corresponding authors. Tel.: +1 781 860 8402 (B.L.); e-mail: blaise.lippa@cubist.com

0960-894X/$ - see front matter © 2008 Elsevier Ltd. All rights reserved.
doi:10.1016/j.bmcl.2008.04.034

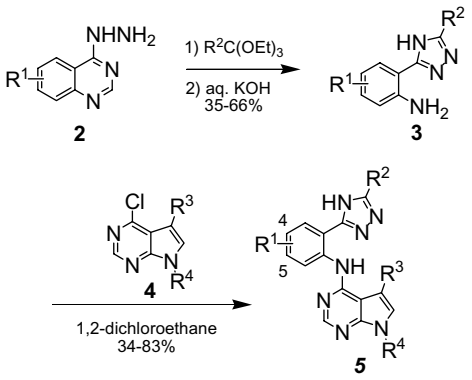

Scheme 1. The synthesis of anilinotriazole pyrrolopyrimidine analogs.

Table 1. Akt1 kinase potency of anilinotriazole analogs **1** and **5a–f**

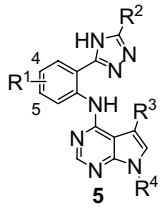

Compound	R^1	R^2	R^3	R^4	Akt1 kinase IC_{50}[a] (nM)
1	H	H	H	H	210 ± 66
5a	H	H	H	**Me**	>10,000
5b	H	H	**Me**	H	425 ± 112
5c	H	H	**Cl**	H	318 ± 86
5d	H	**Me**	H	H	151 ± 32
5e	**4-Cl**	**Me**	H	H	171 ± 51
5f	**5-Cl**	**Me**	H	H	>10,000

[a] Values are means of at least two experiments.

nitrogen (**5a**) resulted in a complete loss of activity, suggesting that this NH and the adjacent pyrimidine nitrogen may be forming a key donor–acceptor hydrogen bonding interaction with the hinge region of the protein, common among kinase inhibitors. Substitution at the C5 position on the pyrrolopyrimidine nucleus with either methyl or chloro was tolerated (**5b**, **5c**), as was methyl substitution at R^2 of triazole (**5d**). SAR on the linking phenyl ring showed more divergent SAR. While a Cl group was tolerated at the 4 position (**5e**), a Cl group at the 5 position resulted in >10 μM inhibition of Akt1 (**5f**).

Subsequently, an X-ray co-crystal structure of analog **5d** bound to the kinase domain of Akt1 was generated (Fig. 2).[23] This structure confirmed that the pyrrolopyrimidine was in fact acting as a hydrogen bond donor–acceptor in binding to the hinge region of Akt1. The crystal structure further reveals that the triazole is forming two hydrogen bonds to adjacent waters and is pi stacking with phenylalanine 161. Importantly, the solved structure also showed a tight intramolecular hydrogen bond between the aniline NH and one of the triazole nitrogens. This observation suggested that additional rigidity could be introduced into the molecule by replacement of this hydrogen bond with a covalent bond, resulting in a new ring, and possibly improved potency. In designing new analogs of this type, it was also deemed important to preserve the intermolecular hydrogen bonds that the triazole makes with bound waters. With these design criteria in mind, imidazopiperidine analogs were targeted.

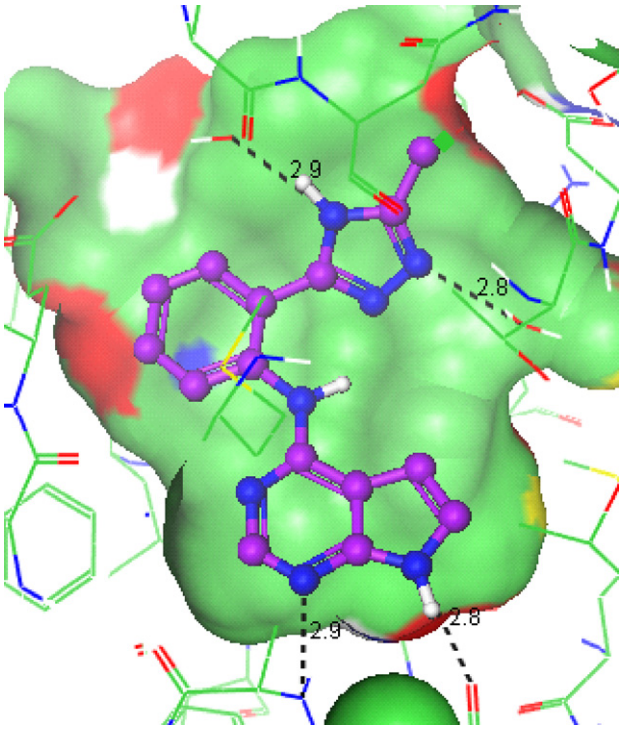

Figure 2. X-ray co-crystal structure of triazole **5d** bound to Akt1.

Scheme 2 illustrates the synthesis of imidazopiperidines **8a** and **8b**. Histamine (**6**) is condensed with paraformaldehyde in refluxing water to form imidazopiperidine **7**.[24] The amine is then added to chloropyrrolopyrimidine (**4**) in low yield (unoptimized) to obtain the final analogs. Imidazopiperidine analog **8a** inhibited Akt1 with similar potency as triazole **1** (294 ± 80 nM). However, in this series chlorine substitution at C5 of the pyrrolopyrimidine provided a 7-fold boost in potency (**8b**: 42 ± 30 nM), representing a key potency lead in antagonizing Akt1. This substituent effect is divergent from the

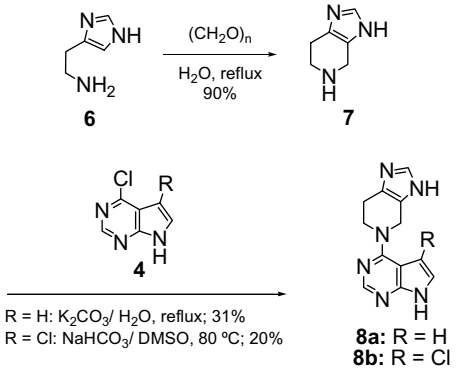

Scheme 2. Synthesis of imidazopiperidine analogs.

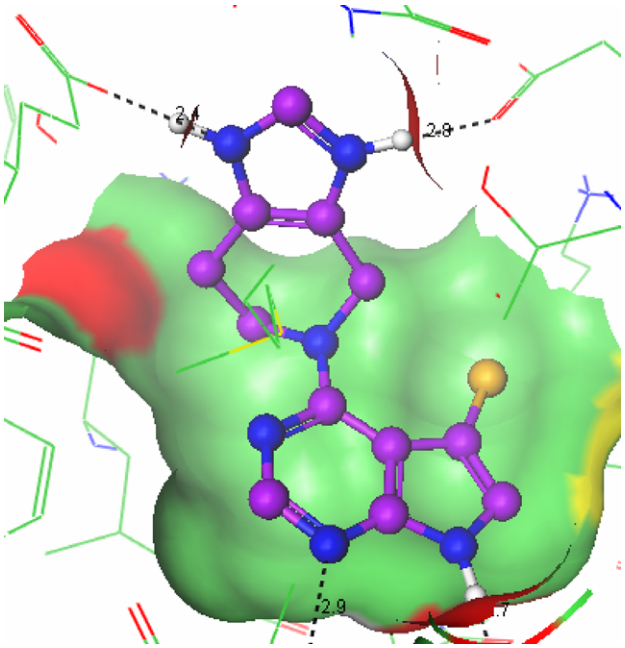

Figure 3. X-ray co-crystal structure of imidazopiperidine **8b** bound to Akt1.

triazole series SAR where a C5 substituent provided no boost in potency (**1** vs **5b**, **5c**).

To better understand the binding of imidazopiperidines to Akt, an X-ray co-crystal structure of **8b** was solved (Fig. 3).[23] While the pyrrolopyrimidine portion of **8b** bound nearly identically with that of **5d** (Fig. 2), the region around the imidazopiperidine showed large changes. Most notably, the protonated imidazole nitrogens are still involved in two hydrogen bonds, but instead of binding to bound waters, they are binding to glutamate 234 and aspartate 292 in the vicinity of where the ribose of ATP would normally occupy. In addition, phenylalanine 161, which pi stacked with the triazole of **5d**, is now swung outward resulting in a significant conformational change in this portion of the protein.

From an SAR perspective, the enhanced potency of this cyclized amine moiety suggested the need to more broadly explore analogs incorporating this functionality. Toward this goal, a diverse set of amines were appended to chloropyrrolopyrimidines **4**, and from this effort spiroindolines (**13**, Scheme 3) were identified as potent inhibitors. Analogs of this type contain a cyclic amine fused to a phenyl group. The cyclic amine of **13** is expected to overlap well with the piperidine of imidazopiperidine **8**, whereas the fused phenyl ring is expected to overlap well with the phenyl of triazole leads (**1**, **5**). The distal spiro-piperidine amine of **13** is expected to bind in the region of the imidazole/triazole, and thus form hydrogen bonds with the polar residues in this portion of the Akt1 binding pocket.

Compounds of this type were synthesized through the addition of optionally substituted hydrazines (**9**) with the protected aldehyde **10** (Scheme 3).[25] Cyclization followed by reduction with sodium borohydride resulted in

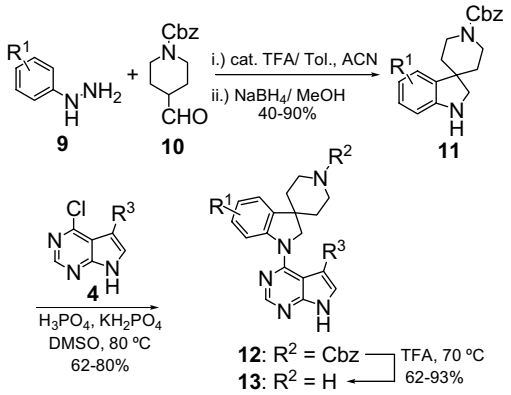

Scheme 3. Synthesis of spiroindoline analogs.

spiroindoline **11**. Addition of this intermediate to chloropyrrolopyrimidine **4** initially proved challenging. Although a melt at high temperatures with these reagents provided product, it was often low yielding and not reproducible. Subsequently, it was found that acid catalysis in DMSO gave improved yields, presumably through the protonation of the pyrimidine resulting in an increase in the electrophilicity of the heterocycle. However, particularly with cyanide substituents, acid catalysis along with the HCl generated in the reaction as a by-product led to decomposition and low yields. An optimum procedure was developed using phosphoric acid to catalyze the reaction in the presence of KH_2PO_4 as a buffer to consume the HCl by-product. This procedure resulted in yields of 62–80% across a wide range of substrates.

The unsubstituted spiroindoline **13a** proved to be a very potent Akt inhibitor, with 5.3 ± 0.9 nM kinase potency,[20] and 96 ± 9 nM cell potency[26] (Table 2). This lead was tolerant to substituents at R^1 on the phenyl ring (**13b**, **13c**), similar to the triazole series (**5e**). Separately, while a methyl R^2 substituent on the piperidine of the spiroindoline was relatively well tolerated (**13d**), functionality that reduced the basicity of the piperidine nitrogen (**13e**, **13f**) was significantly deleterious to activity. Substitution at C5 on the pyrrolopyrimidine (R^3) revealed that chloro (**13g**) and methyl (**13h**) substitution was tolerated. This SAR is similar to the triazole series (**5b**, **5c**), but different from the imidazopiperidine series (**8b**) where chlorine substitution led to a large increase in potency. In the spiroindoline series, further increases in bulk at R^3 to Bn (**13i**) caused a large drop in potency, whereas cyanide **13j** was well tolerated with a kinase IC_{50} of 2.4 ± 0.6 nM and cell potency of 50 ± 19 nM.[27] Compounds in all series showed little kinase selectivity over the closely related PKA. For instance, **13j** inhibits PKA with an IC_{50} of 3.6 ± 2.2 nM, under identical conditions.

Given the impressive activity profile and ligand efficiency[28] of **13j**, it was further studied to determine its in vivo anti-tumor and pharmacokinetic properties. Mice xenografted with a Rat-1a tumor line activated with human myristilated Akt1 (Myr-Akt1) were given 50 mg/kg doses of **13j** for 10 days orally. This treatment

Table 2. Akt kinase and cell potency of spiroindolines **13a**– **j**

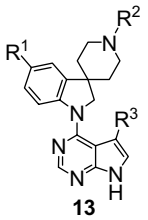

13

Compound	R^1	R^2	R^3	Akt1 kinase IC_{50}[a] (nM)	Akt cell IC_{50}[a] (nM)
13a	H	H	H	5.3 ± 0.9	96 ± 9
13b	Cl	H	H	4.8 ± 1.2	51 ± 33
13c	F	H	H	3.1 ± 1.9	75 ± 6
13d	H	Me	H	12.7 ± 11.0	136 ± 3
13e	F	COMe	H	2790 ± 318	NT
13f	F	SO_2Me	H	3190 ± 346	NT
13g	H	H	Cl	5.8 ± 4.9	64 ± 49
13h	H	H	Me	4.8 ± 3.9	122 ± 19
13i	H	H	Bn	1330 ± 572	NT
13j	H	H	CN	2.4 ± 0.6	50 ± 19

[a] Values are means of at least two experiments; NT, not tested.

resulted in tumor growth inhibition of 68% versus control, with plasma C_{max}, C_{ave} and total daily AUC concentrations of 705 ng/mL, 402 ng/mL, and 3216 ng h/mL, respectively.

In conclusion, the use of structure based drug design aided in the optimization of a high throughput screening hit, resulting in the design of several new series and a ~100-fold increase in Akt1 inhibition. Compound **13j** was further shown to inhibit Akt in cells, and to slow the growth of tumors in vivo. Kinase selectivity remains a key concern. Further results in optimizing kinase selectivity, Akt potency, and drug-like properties will be published in due course.

Acknowledgments

Michael Luzzio, Kevin Freeman-Cook, Chiliu Chen, Christopher Autry, Catherine Hulford, Kendra Nelson, Gary Martinelli, Donn G. Wishka, Matthew Marx, Yong Lu, Martin Wythes, Chakrapani Subramanyam, William Hungerford, Jinshan Chen, Shang-Poa Chang, Joel Arcari, Tricia Kwan, Carl Thompson, and Aaron Kanter provided additional chemistry support. Additional biology support was received from Kevin Coleman, Kristina Rafidi, Kou Kou, Jing Lin, Erik Soderstrom, and Lili Yao.

References and notes

1. Bellacosa, A.; Franke, T. F.; Gonzalez-Portal, M. E. *Oncogene* **1993**, *8*, 745.
2. Fayard, E.; Tintignac, L.; Baudry, A.; Hemmings, B. *J. Cell Sci.* **2005**, *24*, 7455.
3. Altomare, D. A.; Testa, J. R. *Oncogene* **2005**, *24*, 7455.
4. Borzillo, G. V. *Drug Discov. Today: Ther. Strateg.* **2005**, *2*, 331.
5. LoPiccolo, J.; Granville, C. A.; Gills, J. J.; Dennis, P. A. *Anti-Cancer Drugs* **2007**, *18*, 861.
6. Samuels, Y.; Ericson, K. *Curr. Opin. Oncol.* **2006**, *18*, 77.
7. Carpten, J. D.; Faber, A. L.; Horn, C.; Donoho, G. P.; Briggs, S. L.; Robbins, C. M.; Hostetter, G.; Boguslawski, S.; Moses, T. Y.; Savage1, S.; Uhlik, M.; Lin, A.; Du, J.; Qian, Y.-W.; Zeckner, D. J.; Tucker-Kellogg, G.; Touchman, J.; Patel, K.; Mousses, S.; Bittner, M.; Schevitz, R.; Lai, M.-H. T.; Blanchard, K. L.; Thomas, J. E. *Nature* **2007**, *448*, 439.
8. Pedrero, J. M. G.; Carracedo, D. G.; Pinto, C. M.; Zapatero, A. H.; Rodrigo, J. P.; Nieto, C. S.; Gonzalez, M. V. *Int. J. Cancer* **2005**, *114*, 242.
9. Li, Q. *Expert Opin. Ther. Patents* **2007**, *17*, 1077.
10. Lindsley, C. W.; Barnett, S. F.; Yaroschak, M.; Bilodeau, M. T.; Layton, M. E. *Curr. Topics Med. Chem.* **2007**, *7*, 1349.
11. Lindsley, C. W.; Zhao, Z.; Leister, W. H.; Robinson, R. G.; Barnett, S. F.; Defeo-Jones, D.; Jones, R. E.; Hartman, G. D.; Huff, J. R.; Huberb, H. E.; Duggan, M. E. *Bioorg. Med. Chem. Lett.* **2005**, *15*, 761.
12. Kozikowski, A. P.; Sun, H.; Brognard, J.; Dennis, P. A. *J. Am. Chem. Soc.* **2003**, *125*, 1144.
13. Zhu, G.-D.; Gandhi, V. B.; Gong, J.; Thomas, S.; Woods, K. W.; Song, X.; Li, T.; Diebold, R. B.; Luo, Y.; Liu, X.; Guan, R.; Klinghofer, V.; Johnson, E. F.; Bouska, J.; Olsen, A.; Marsh, K. C.; Stoll, V. S.; Mamo, M.; Polakowski, J.; Campbell, T. J.; Martin, R. L.; Gintant, G. A.; Penning, T. D.; Li, Q.; Rosenberg, S. H.; Giranda, V. L. *J. Med. Chem.* **2007**, *50*, 2990.
14. Luo, Y.; Shoemaker, A. R.; Liu, X.; Woods, K. W.; Thomas, S. A.; De Jong, R.; Han, E. K.; Li, T.; Stoll, V. S.; Powlas, J. A.; Oleksijew, A.; Mitten, M. J.; Shi, Y.; Guan, R.; McGonigal, T. P.; Klinghofer, V.; Johnson, E. F.; Leverson, J. D.; Bouska, J. J.; Mamo, M.; Smith, R. A.; Gramling-Evans, E. E.; Zinker, B. A.; Mika, A. K.; Nguyen, P. T.; Oltersdorf, T.; Rosenberg, S. H.; Li, Q.; Giranda, V. L. *Mol. Cancer Ther.* **2005**, *4*, 977.
15. Lin, X.; Murray, J. M.; Rico, A. C.; Wang, M. X.; Chu, D. T.; Zhou, Y.; Del Rosario, M.; Kaufman, S.; Ma, S.; Fang, E.; Crawford, K.; Jefferson, A. B. *Bioorg. Med. Chem. Lett.* **2006**, *16*, 4163.
16. Breitenlechner, C. B.; Wegge, T.; Berillon, L.; Graul, K.; Marzenell, K.; Friebe, W.-G.; Thomas, U.; Schumacher, R.; Huber, R.; Engh, R. A.; Masjost, B. *J. Med. Chem.* **2005**, *48*, 163.
17. Lippa, B. *Expert Opin. Ther. Patents* **2007**, *17*, 577.

18. Donald, A.; McHardy, T.; Rowlands, M. G.; Hunter, L.-J. K.; Davies, T. G.; Berdini, V.; Boyle, R. G.; Aherne, W.; Garrett, M. D.; Collins, I. *J. Med. Chem.* **2007**, *50*, 2289.
19. Saxty, G.; Woodhead, S. J.; Berdini, V.; Davies, T. G.; Verdonk, M. L.; Wyatt, P. G.; Boyle, R. G.; Barford, D.; Downham, R.; Garrett, M. D.; Carr, R. A. *J. Med. Chem.* **2007**, *50*, 2293.
20. Akt1 kinase assay: A fluorescence polarization IMAP type assay is used. 15 μL of diluted test compound in DMSO is mixed with 60 μL of reaction buffer (10 mM Tris–HCl, pH 7.5, 10 mM $MgCl_2$, 0.1 mM EGTA, 0.01% Triton X-100, 1 mM DTT). About 5 μL of the compound/buffer mixture, 10 μL of a solution containing 4 μM ATP, and 40 nM fluorescent-labeled Crosstide (Tamara-labeled GRPRT SSFAEG peptide), and 5 μL of Akt1 protein (lacking the pleckstrin homology (PH) domain, containing an Asp at position 473, and pre-phosphorylated at Thr 308) in reaction buffer are combined. After a 90 min incubation, IMAP beads are added and plates are read (lamp filter: 544 nm, emission filter: 615 nm). The same procedure can be applied to full length Akt1 to provide similar results. For example, compound **1** inhibits full length Akt1 with an IC_{50} of 223 ± 110 nM. As expected, no compounds tested have shown Akt isozyme selectivity (Akt1, 2 or 3).
21. Potts, K. T.; Brugel, E. G. *J. Org. Chem.* **1970**, *35*, 3448.
22. Gerster, J. F.; Hinshaw, B. C.; Robins, R. K.; Townsend, L. B. *J. Heterocycl. Chem.* **1969**, *6*, 207.
23. Pandit, J. WO 2005113762A1, 2005; Atomic coordinates and structure factors of the protein structures in this paper have been deposited in the RCSB Protein Data Bank, with accession numbers 3CQU and 3CQW.
24. Habermehl, G. G.; Ecsy, W. *Heterocycles* **1976**, *5*, 127.
25. Maligres, P. E.; Houpis, I.; Rossen, K.; Molina, A.; Sager, J.; Upadhyay, V.; Wells, K. M.; Reamer, R. A.; Lynch, J. E.; Askin, D.; Volante, R. P.; Reider, P. J.; Houghton, P. *Tetrahedron* **1997**, *53*, 10983.
26. Akt cell assay: The phosphorylation status of an Akt substrate, GSK-3α, in the U87 glioblastoma line is measured. Cells were incubated with compound (7 concentrations plus vehicle) for 2 h in DMEM medium lacking fetal calf serum (FCS). After cell lysis, p-GSK-3α was captured on 96-well plates coated with a phosphospecific antibody to GSK-3α/β (#9331, Cell Signaling Technology). The reporter antibody bound total GSK-3α (#SC-5264, Santa Cruz), and was measured in an ELISA format.
27. Unfortunately, it was not possible to obtain high-quality crystal structures on any member of the spiroindoline lead series (**13**).
28. Hopkins, A. L.; Groom, C. R.; Alex, A. *Drug Discov. Today* **2004**, *9*, 430.